Miniaturization of dielectric liquid microlens in package

Chih-Cheng Yang, C. Gary Tsai, and J. Andrew Yeh[a)]
Institute of NanoEngineering and MicroSystems, National Tsing Hua University, Hsinchu 30013, Taiwan

(Received 30 July 2010; accepted 5 September 2010; published online 30 December 2010)

This study presents packaged microscale liquid lenses actuated with liquid droplets of 300–700 μm in diameter using the dielectric force manipulation. The liquid microlens demonstrated function focal length tunability in a plastic package. The focal length of the liquid lens with a lens droplet of 500 μm in diameter is shortened from 4.4 to 2.2 mm when voltages applied change from 0 to 79 V_{rms}. Dynamic responses that are analyzed using 2000 frames/s high speed motion cameras show that the advancing and receding times are measured to be 90 and 60 ms, respectively. The size effect of dielectric liquid microlens is characterized for a lens droplet of 300–700 μm in diameter in an aspect of focal length. © *2010 American Institute of Physics.* [doi:10.1063/1.3494030]

I. INTRODUCTION

Tunable liquid lenses that adjust focal lengths without movable mechanical parts emerge to be adopted in systems that include adaptive lenses,[1] endoscopes,[2] light valves,[3] optical communication systems,[4] and barcode readers.[5] Two actuation approaches, mechanical and electric energy, were applied.[6–10] The electric approaches include electrowetting, electrowetting on dielectrics, and dielectric force;[11–13] however, problems associated with microbubble and Joule heating occur often due to liquid electrolysis and high conductivity of conductive liquid, particularly in electrowetting. The dielectric force attracts interests in eliminating the problems mentioned above.[14,15] Lens droplets made of liquid crystals suffer from birefringement, resulting in utilization of liquids with lower molecule weights. To facilitate the operation of the liquid lens at any positions, the gravitational effect taken into account is proposed to be minimized two liquids of isodensity.[16,17]

The aperture diameter of a tunable focal length liquid lens ranges typically from a few millimeters to centimeters. Miniaturization of the liquid lenses can be further applied to the integrated or compact micro-optical systems, such as endoscopes, fiber optics, and security cameras and optical sensors. Until now, there exist several issues to be solved all together, including precise liquid dispensing, centering of optic axis, microscale actuation mechanism, and device packaging. It is critical to precisely manipulate the volume of droplet dispensing due to its effect on initial lens profiles (i.e., initial contact angles of lens droplets). The liquid microlens encounters drift of liquids, leading to unstable optic axis at the rest state and during actuation.[1,12] A cavity-shaped polymer on indium tin oxide electrode was proposed but image resolution still remains a question due to structures where light passes through. Unlike macroscale liquid lenses, voltage-effective design is required to actuate the liquid microlens. Electrode designs studied, such as parallel plate electrodes with holes and pure parallel plate electrodes, require high voltage biases of nearly 100 V to achieve a focal length change by 50%. Finally, device packaging is rarely reported in fabrication of the liquid microlens.

This study presents the characterizations of a dielectric liquid microlens with plastic packaging that attempts to simultaneously tackle the problems mentioned above. The liquid microlens was investigated with a lens droplet of several hundred micrometers in diameter. Optical images

[a)]Author to whom correspondence should be addressed. Electronic mail: jayeh@mx.nthu.edu.tw.

are clearly captured using the packaged liquid microlens. Planar liquid confinement structures along with concentric electrodes are used for optical centering of the dielectric liquid microlens at the rest state and during actuation. Plastic package structure is used to seal the liquid lenses. The liquid microlens is comprised of two nonconductive (i.e., dielectric) liquids of isodensity, liquid confinement structures, concentric electrodes, and plastic packaging. The dielectric force is induced on interfacial surface when the nonconductive liquids with different dielectric constants are exercised under electric fields. The combination of the liquid confinement structures and the concentric electrodes keeps track of the optical axis alignment at the rest state and during actuation. A size effect was also evaluated for focal length from 300 to 700 μm.

II. MECHANISM AND THEORETICAL ANALYSIS

Figure 1(a) shows a liquid microlens during rest state. A liquid droplet with lower dielectric constant (e.g., silicone oil) is surrounded by a sealing liquid with a higher dielectric constant (e.g., polyalcohol). The droplet spreads to the edge effect of an elevated confinement structure and is then confined by its geometric effect. The two liquids have approximately the same gravitational density. The dielectric force is generated by nonuniform electric fields produced by a set of concentric electrodes. When voltage is applied, the electrodes generate nonuniform electric field to create a dielectric force by polarization effects on droplet surface. Thus, the liquid droplet changes its surface profile. This profile change shortens the focal length, as depicted in Fig. 1(b).

The profile change of the droplet can be described mathematically based on the equilibrium of the steady-state surface free energy, including surface tension, the dielectric force, and gravity effect, using the augmented Young–Laplace equation.[18] The gravitational effect can be estimated by Bond number (B_o), which is defined as the ratio of the gravitational pressure to the pressure difference due to interfacial surface tension,

$$B_o = \frac{\Delta(\rho g z)}{\gamma / R}, \tag{1}$$

$$\gamma\left(\frac{2}{R}\right) = \Delta P_0 + \Delta(\rho g z) + \Delta P_e, \tag{2}$$

where γ is the interfacial surface tension, ρ is the density, R is the principle radius of the droplet curvature, ΔP_o is the interface pressure difference, $\Delta(\rho g z)$ is the gravitational pressure difference, and ΔP_e is the electric pressure difference.

In this study, an interfacial surface tension γ is 0.02 N/m, and a gravity constant g equals to 9.81 m/s^2. The droplet has the a principle radius R of 500 μm at the rest state. Given $\Delta\rho$ of 20 kg/m^3 and the maximum height Z_{max} of 150 μm at actuation by a bias of 79 V_{rms}, the principle radius and the maximum height become 440 μm and 90 μm, respectively. The Bond number is estimated to be smaller than 0.0006. This noteworthy result indicates that droplet deformation due to gravitational pressure is negligible compared to that caused by the interfacial surface in this case. Therefore, surface tension and electric force are dominant in this scale.

The ANSOFT 3D MAXWELL 11.1 simulation package is used to investigate a dielectric force induced by gradient electric fields on the surface of the droplet. The initial profile was experimentally validated using a contact angle image system. The droplet images captured were implemented as boundary conditions in the simulation. The parameters used in this simulation to calculate electric field include a voltage bias of 10 V, an electrode width of 15 μm, an electrode gap of 5 μm, and a droplet of 500 μm in diameter. The droplet with a dielectric constant (ε) of 2 is surrounded by mixed-alcohol with a dielectric constant (ε) of 45. The relative dielectric constant was measured using a high frequency liquid dielectric constant meter (Zadow electronics, ALPHA TDR-5000).

Electric field simulations are shown in Fig. 2. The strength of the electric field in the droplet

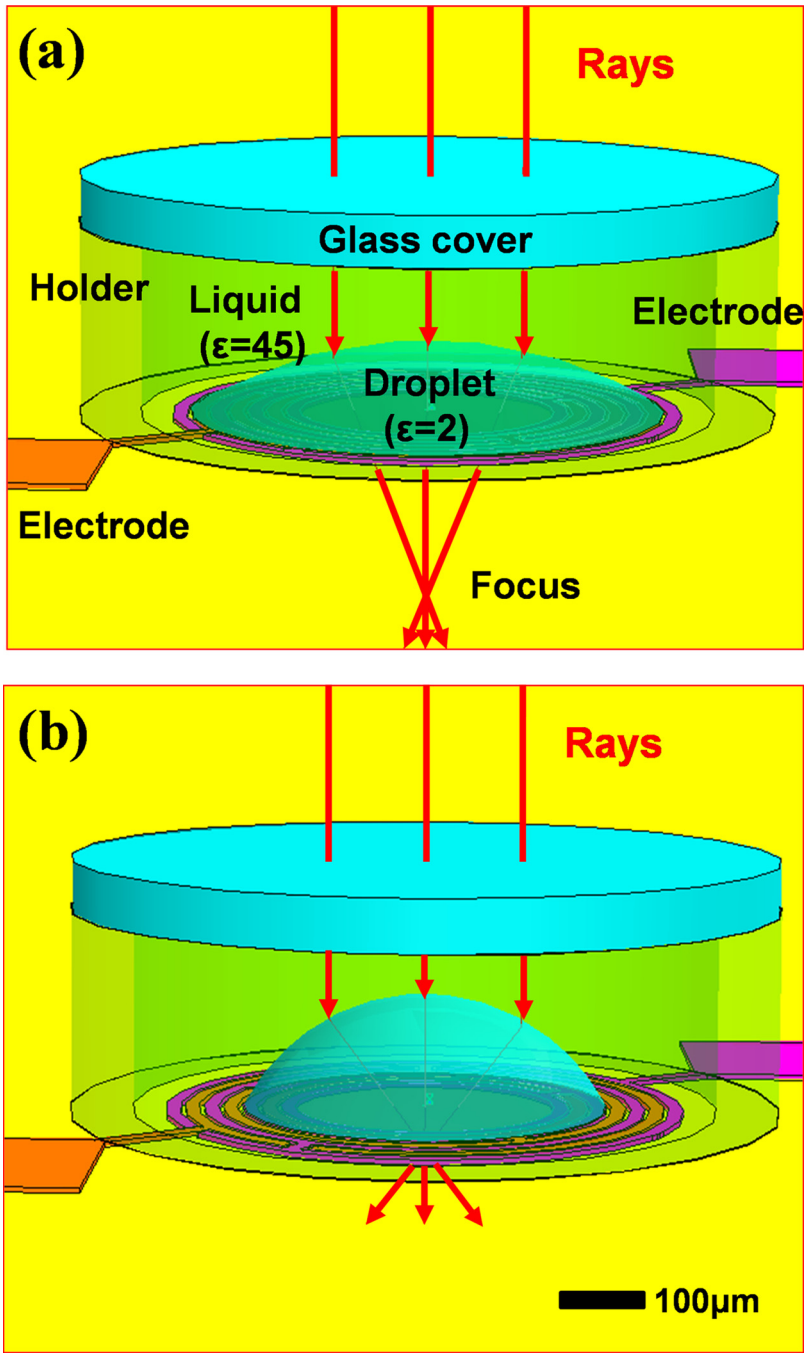

FIG. 1. Schematic of a dielectric liquid microlens (a) at the rest state and (b) at a voltage applied (i.e., contact angle change). The focal lengths of the dielectric liquid microlens change as voltages applied.

decreases dramatically from the electrodes to the top of the droplet. The nonuniform electric field generates a dielectric force toward the region of the liquid with a low dielectric constant, which is imposed on the interface between the two liquids. The magnitude of the force reaches maximum near the contact line [see Fig. 2(b)] due to the nonuniform electric field distribution, as shown in Fig. 2(a). As a result, the droplet is pushed inward and upward since the dielectric forces near the

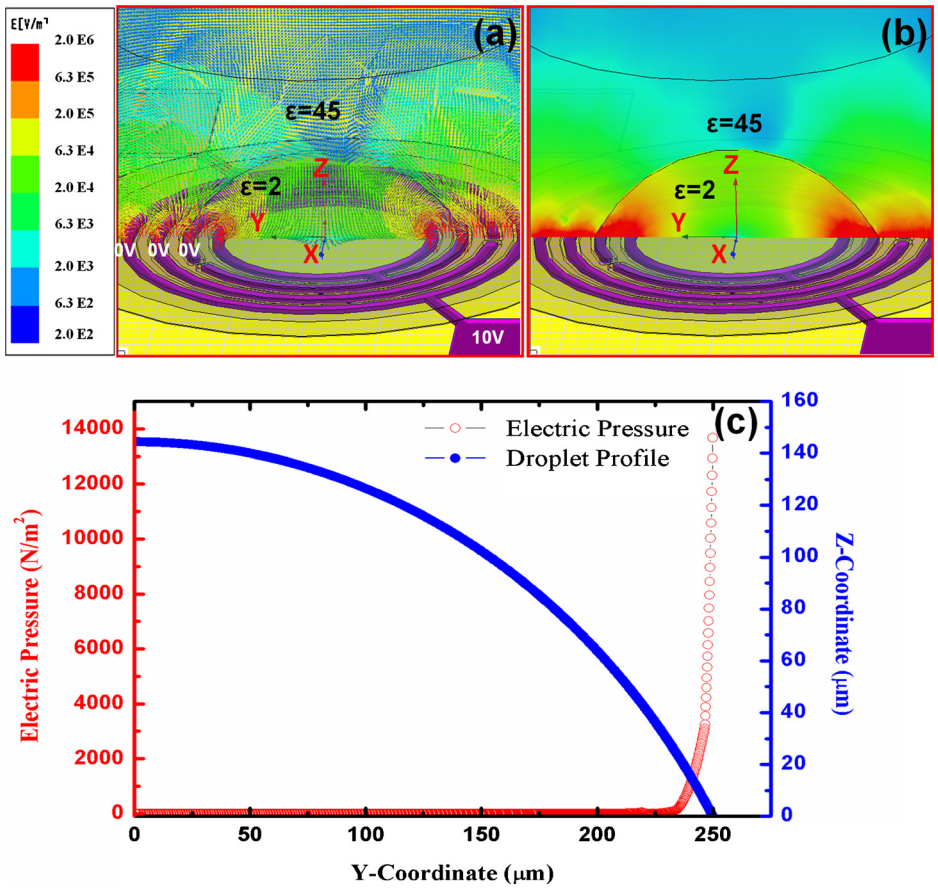

FIG. 2. A simulation of the electric field of a liquid droplet includes a voltage bias of 10 V, an electrode width of 15 μm, and with a electrode gap of 5 μm on a droplet of 500 μm in diameter. (a) Cross section of the distribution of the electric field vector. (b) Cross section of the magnitude of the electric field. (c) Electric pressure generated by dielectric force along droplet surface.

electrodes are larger than those at the top of the droplet by several orders. As the droplet is squeezed, the contact angle increases. Electric force distribution was calculated using the electric fields exported from the simulations.

Figure 2(c) shows that the electric pressure (i.e., the dielectric force divided by a unit surface area) along the droplet surface is calculated from simulation.

III. DEVICE FABRICATION AND EXPERIMENTS

A. Device fabrication

A 0.5 μm thick aluminum layer was deposited onto a 0.55 mm thick glass substrate using an e-gun evaporator, lithographically patterning and wet etching concentric electrodes. A 1 μm thick SU-8 layer was coated as an insulating layer. Shape patterns of hydrophilic resin and hydrophobic Teflon were photolithographically fabricated onto the SU-8 layer. The liquid droplet of the micro-lens was confined by the Teflon pattern and sealed by the other liquid inside a plastic holder, as shown in Fig. 3(a). The high dielectric and low dielectric liquids have refractive indices of 1.49 and 1.39, respectively. An UV cure adhesive is used to seal the gaps. Figure 3(b) shows that an UV cure adhesive provides adhesion between bottom glass substrate patterned aluminum electrodes and plastic holder. An UV cure adhesive is subsequently painted on the area of holder where top glass will cover. Afterward, the holder is put inside a vessel which is full of polyalcohol. After the oil droplet is confined, top glass is glued. The UV light is used for fast curing UV adhesive to seal

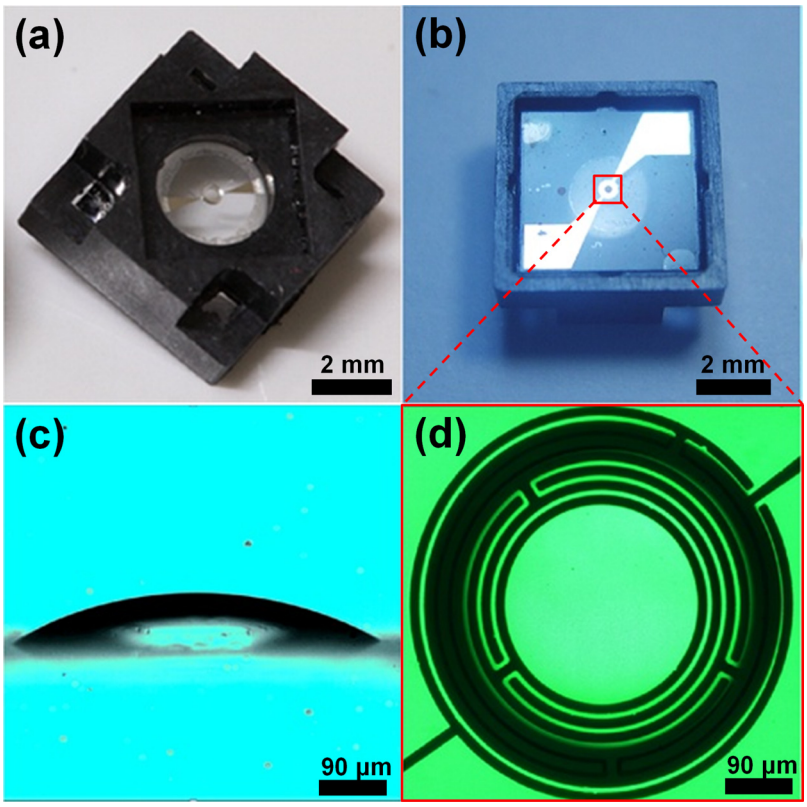

FIG. 3. (a) Top view of packaged liquid microlens with a glass cover on the top of plastic holder. (b) Photo capture of fabricated device from backside of packaged liquid microlens. (c) Side view of a microlens captured by contact angle measurement system at the rest state condition. (d) Top view of a liquid droplet sitting on the top of electrodes with a transparent aperture at the center captured by microscope digital camera.

the top glass. In Fig. 3(c), the side view of the liquid microlens is imaged with a contact angle meter (Sindatek Model 100SB). The liquid microlens with a 500 μm diameter has a spherical shape when no voltage is applied. To investigate the focal length of the liquid microlens, the electrodes were fabricated with a transparent aperture at the center, as shown in Fig. 3(d). Note that the packaged liquid microlens is designed for future optical sensing application used.

B. Experimental setup

An optical microscope (OLYMPUS Inverted Microscope IX71) was used to observe the focal length of a dielectric liquid microlens. The focal length of liquid microlens could be measured from transparent light focused on objective lens through finding a clear image. The images were captured using a Charge Coupled Device (CCD) sensor array connected to the output port of the microscope. The focal plane of liquid microlens was modified when different voltage applied.

The experimental setup of a contact angle measurement system (Sindatek Model 100SB) is shown in Fig. 4. The measurement system consists of a camera, an illuminator, high-performance zoom telescope, and image analysis software system. The static and dynamic contact angle analysis system was conducted for a dielectric liquid microlens.

A digital camera capable of 30 frames/s was used for static contact angle observation. For dynamic observation, the images were captured with a speed of 2000 frames/s at a resolution of 1024×1024 using a high speed camera (Redlake MotionXtra camera Y4). The images were stored in a computer via a USB cable between the camera and the computer. The images were later

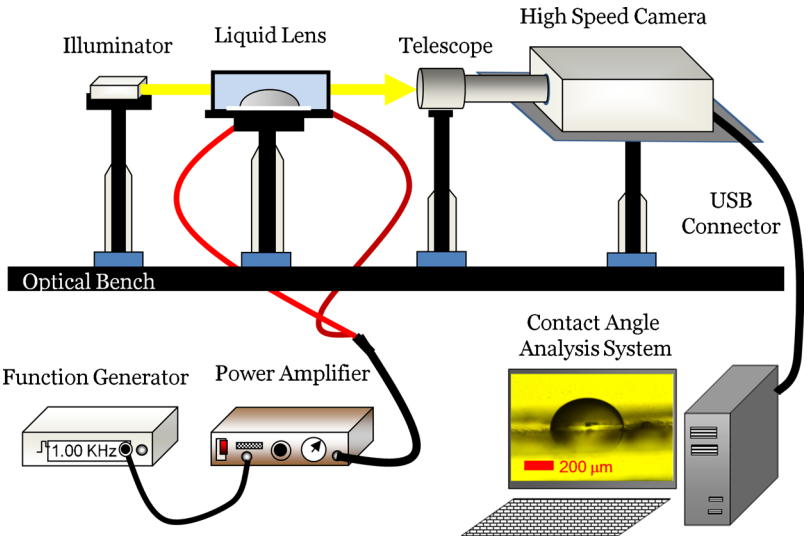

FIG. 4. A schematic diagram of experimental setup used to measure contact angle. The contact angle was calculated from photograph of the droplet profile.

processed by MotionPro Data Acquisition System (Motion studio software, IDT, Inc., Florida, USA). The information of the advancing, receding, and time index was compared to analyze the key characteristics of dynamic and static angles of liquid microlens.

An ac high voltage amplifier power supply (A-303 Piezo Modulator, SUPEREX Technology, Taiwan) along with a function generator (Model 33220A, Agilent) was used to apply electric potentials on a dielectric liquid microlens.

C. Characterizations of dielectric liquid microlens

An optical microscope was used to observe the variation of focal length of two rows of letters when different voltages applied. The two rows of letters were imaged at various focal lengths created by varying the voltages between 0 and 79 V_{rms} (see Fig. 5). The letters of magnification in the captured images were a function of the microlens focal length through different voltages applied on liquid microlens. An effect of tunable focal length was demonstrated. One of the advantages of the dielectric liquid microlens is the power consumption. The power consumption was measured to be 0.4 mW at the condition of an applied voltage of 79 V_{rms} and a measured current of 26 μA.

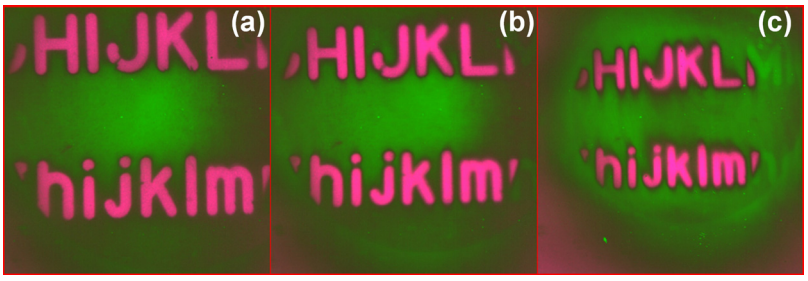

FIG. 5. Two rows of letters were imaged at various focal lengths of microlens with a diameter of 500 μm. The images were captured with (a) 0 V, (b) 43 V_{rms}, and (c) 79 V_{rms} applied voltage on electrodes.

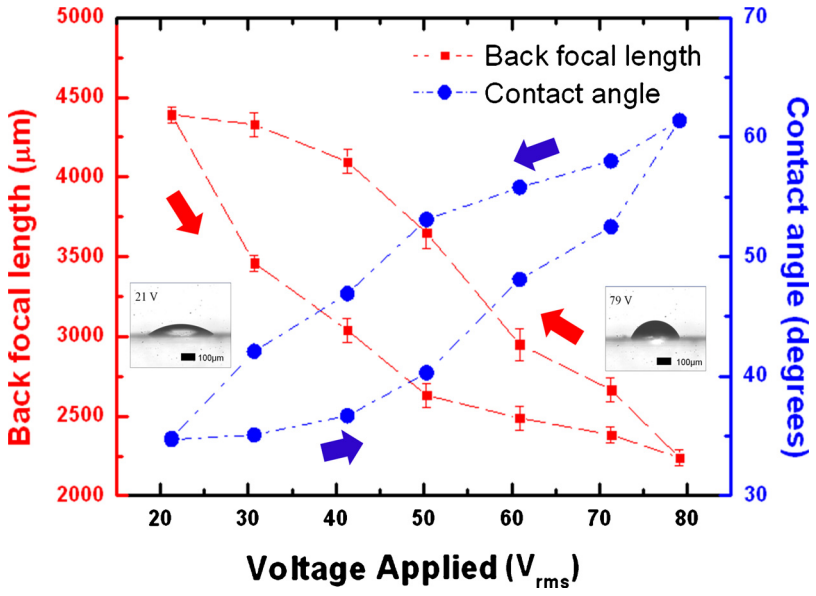

FIG. 6. Static responses of liquid microlens were measured for the back focal length and contact angles vs the 500 μm diameter when a voltage was applied from 0 V to 79 V_{rms}.

Figure 6 shows the static response of a dielectric liquid microlens with respect to voltages applied, including focal length and contact angle. The contact angle was measured using a contact angle meter (Sindatek Model 100SB). When voltage applied varies from 0 to 79 V_{rms}, the measured contact angle increases from 35° to 61° and the focal length decreases from 4400 to 2200 μm. The observed hysteresis effect shows different paths of the dielectric liquid microlens in the advancing stage and in the receding stage. The focal length returns to the original one after a cycle of operation. The fitting conic constants of the profiles at the rest state and at 79 V_{rms} are calculated to -0.02 and 0.02, respectively. Such values of conic constants imply that the liquid lens remains spherical at these two equilibrium states. In other words, one can treat liquid microlens in this scale as spherical lenses with variable focal lengths. The variable focal length for liquid lens can be theoretically calculated from the basic lens maker's formula.[19] The results of calculated focal length are 4392 μm and 2800 μm at the contact angle of 35° and 61°, respectively. The results have a good agreement with measurement focal length.

Figure 7 displays the dynamic responses of the liquid microlens when 79 V_{rms} at 1 kHz voltage was applied. Dynamic responses of a liquid droplet with 500 μm in diameter were studied. The images were captured with a speed of 2000 frames/s at a resolution of 1024×1024 pixels using a high speed motion camera (Redlake MotionXtra camera Y4). Image software (Sindatek Model 100SB MagicDroplet) was used to analyze the images with curve fitting and contact angle calculation. The conic approach model was chosen to match the microlens profile. For a microlens with a diameter of 500 μm, the advancing time and the receding time were measured to be 90 ms and 60 ms, respectively, given a voltage of 79 V_{rm} applied.

Figure 8 illustrates the size effect by investigating the change of back focal length when voltage is applied upon different diameters of dielectric liquid microlens. The sizes of droplets from 300 to 700 μm in diameter were used to investigate the size effect. The same initial contact angle was used in this measurement. The back focal lengths of dielectric liquid microlens decrease gradually with increasing applied voltage. By comparing the back focal length at the initial condition (i.e., no applied voltage) with the one at applied 79 V_{rms}, the back focal lengths of liquid microlens decrease by 22%, 35%, and 41% relative to the size of 700 μm, 500 μm, and 300 μm in diameter, respectively. The smaller size of dielectric liquid microlens has more relative change of back focal lengths when 79 V_{rms} applied.

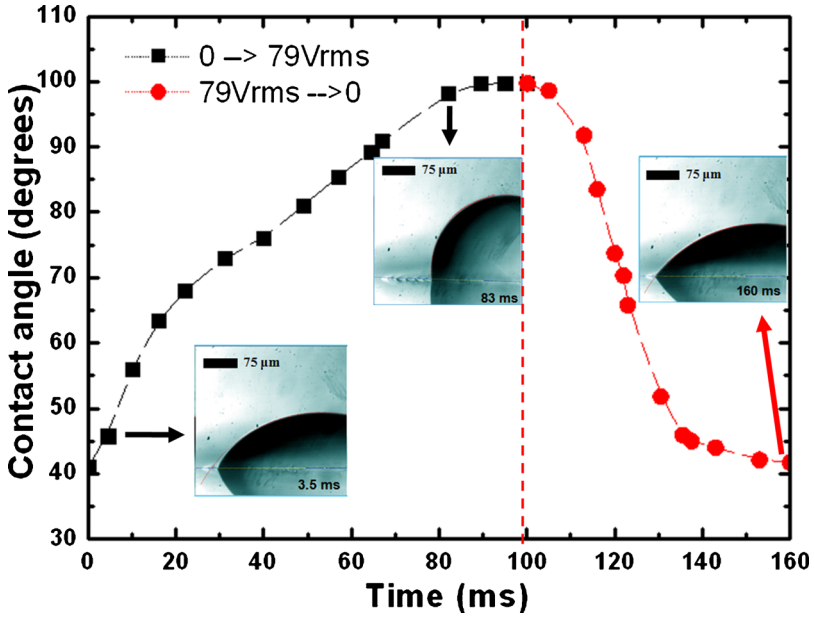

FIG. 7. Dynamic responses of liquid microlens with a diameter of 500 μm captured at a speed of 2000 frames/s when a 79 V_{rms} at 1 kHz voltage was applied. The surface profiles were curve fitted using conic model. The dynamic responses of advancing and receding states were recorded using high speed motion camera.

IV. CONCLUSIONS

A packaged dielectric liquid microlens was demonstrated in this study. Packaging the dielectric liquid microlens was performed using a plastic holder. The characterizations of dielectric liquid microlens with a diameter of 500 μm were investigated, including focal lengths, images, and static and dynamic responses at various applied voltage states. The size effect experiment

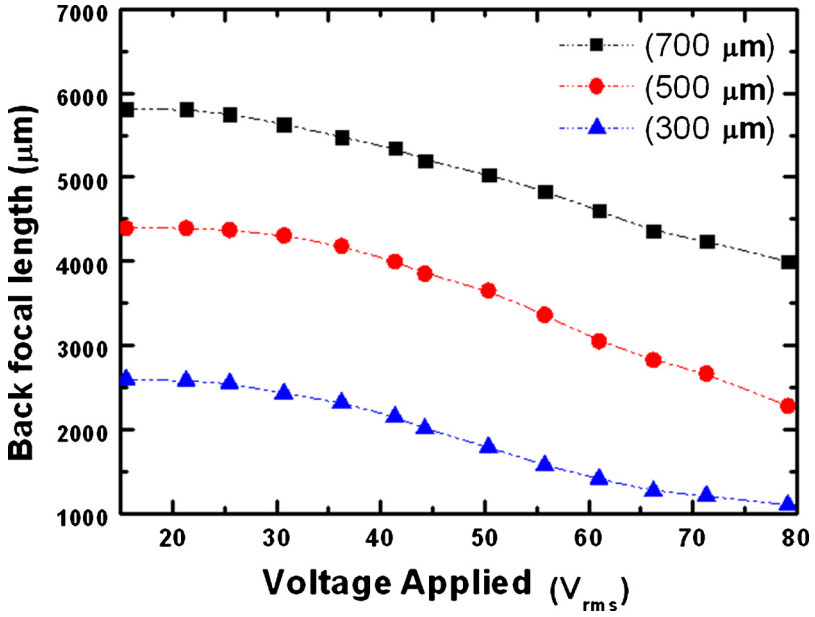

FIG. 8. Illustrates the size effect by investigating the dependence of the back focal lengths of different diameters of dielectric liquid microlens when voltage is applied upon electrodes.

indicated that a dielectric liquid microlens with a smaller size led to more relative change of back focal length for the lens droplets from 300 to 700 μm in diameter. The package of the liquid microlens was designed to be integrated with another optical device for motion sensing applications in the near future.[20]

ACKNOWLEDGMENTS

This work has been financially supported by the National Science Council, Republic of China under Grant Nos. NSC 96-2628-E-007-124-MY3 and NSC 98-2218-E-007-004. Help from Chong-Yao Yang for photograph is appreciated.

[1] H. Ren, H. Xianyu, S. Xu, and S. T. Wu, Opt. Express **16**, 14954 (2008).
[2] D. Y. Zhang, V. Lien, Y. Berdichevsky, J. Choi, and Y. H. Lo, Appl. Phys. Lett. **82**, 3171 (2003).
[3] J. Heikenfeld and A. J. Steckl, Appl. Phys. Lett. **86**, 151121 (2005).
[4] H. Ren, Y. H. Fan, and S. T. Wu, Opt. Lett. **29**, 1608 (2004).
[5] Z. He, T. Nose, and S. Sato, Jpn. J. Appl. Phys., Part 1 **34**, 2392 (1995).
[6] W. Wang, J. Fang, and K. Varahramyan, IEEE Photon. Technol. Lett. **17**, 2643 (2005).
[7] F. S. Tsai, S. H. Cho, Y. H. Lo, B. Vasko, and J. Vasko, Opt. Lett. **33**, 291 (2008).
[8] S. Xu, Y. J. Lin, and S. T. Wu, Opt. Express **17**, 10499 (2009).
[9] U. Levy and R. Shamai, Microfluid. Nanofluid. **4**, 97 (2008).
[10] U. C. Yi and C. J. Kim, J. Micromech. Microeng. **16**, 2053 (2006).
[11] R. A. Hayes and B. J. Feenstra, Nature (London) **425**, 383 (2003).
[12] H. Ren and S. T. Wu, Opt. Express **16**, 2646 (2008).
[13] S. W. Walker and B. Shapiro, J. Microelectromech. Syst. **15**, 986 (2006).
[14] C. C. Cheng, C. A. Chang, C. H. Liu, and J. A. Yeh, J. Opt. A, Pure Appl. Opt. **8**, S365 (2006).
[15] C. C. Cheng, C. A. Chang, and J. A. Yeh, Opt. Express **14**, 4101 (2006).
[16] C. C. Cheng and J. A. Yeh, Opt. Express **15**, 7140 (2007).
[17] C. G. Tsai, C. N. Chen, L. S. Cheng, C. C. Cheng, J. T. Yang, and J. A. Yeh, IEEE Photon. Technol. Lett. **21**, 1396 (2009).
[18] A. Bateni, S. S. Susnar, A. Amirfazli, and A. W. Neumann, Microgravity Sci. Technol. **16**, 153 (2005).
[19] I. Gatland, Am. J. Phys. **70**, 1184 (2002).
[20] W. Iwasaki, H. Nogami, E. Higurashi, and R. Sawada, IEEJ Trans. Electron. Eng. **5**, 137 (2010).